

Mechanical Behavior of Injection-molded Starch-based Polymers

Rui L. Reis,^{1,2} António M. Cunha,³ Peter S. Allan⁴ and Michael J. Bevis⁴

¹ Department of Metallurgical Engineering, FEUP, Rua dos Bragas, 4099 Porto Codex, Portugal

² INEB, Institute for Biomedical Engineering, Praça Coronel Pacheco 1, 4050 Porto, Portugal

³ Department of Polymer Engineering, University of Minho, Azurém, 4800 Guimarães, Portugal

⁴ The Wolfson Centre for Materials Processing, Brunel University, Uxbridge, Middlesex UB8 3PH, UK

ABSTRACT

This work evaluates the mechanical performance of injection-molded starch-based copolymers, 60/40 (mol/mol) starch:poly(ethylene vinyl alcohol), and the possibility of improving material properties through deliberately induced anisotropy during processing. Different types of samples were produced by conventional and shear-controlled injection molding (Scorim) and tested under tensile and impact loading. The behavior of three distinct grades is discussed in terms of the respective fracture morphology (evaluated by scanning electron microscopy). A comparison is made between the behavior of conventional and Scorim samples. The results show that the mechanical properties of the materials used were significantly improved by the employment of the Scorim process. The stiffness values of the conventional moldings were doubled, without reducing the ductility of the polymer. The impact data showed a material sensitivity, and consequent loss of properties, to the localized shear imposed to the melt during processing. This situation is attributed to very narrow mold gates (in the case of pin-gated systems) and leads to much reduced impact performance.

KEYWORDS: starch-based polymers; biomaterials; injection molding; Scorim; impact performance

INTRODUCTION

The use of biodegradable polymers in load-bearing parts for biomedical applications is a promising

This paper is based on an Oral Communication presented at PAT'95, Pisa.

route for the development of more efficient non-permanent implants. The possibility of producing implants in bioabsorbable materials, which must compromise adequate mechanical properties and controlled degradation rates by human fluids, can overcome some problems traditionally associated with metallic implants in orthopaedics. In the case of fixation devices, namely bone plates, the use of a material with a modulus close to that of bone leads to a more adequate load-sharing between the bone and the device, contributing to more efficient healing [1, 2], and preventing stress-shielding effects [3].

Some biodegradable polymers are already under clinical use, including polyglycolic acid (PGA), polylactic acid (PLA) and polyhydroxybutyrate (PHB) [4, 5]. A potential alternative is the starch-based polymers that are well-known biodegradable materials [6, 7]. These materials are blends of maize starch

TABLE 1. Raw Materials Used: Trade Names, Melting Temperature (as Determined by DSC Analysis) and Respective MFIs at 170 °C, 49 N

| Code | Trade name | Melting temperature (°C) | MFI (170°C, 49 N) (g/600 sec) |
|--------|-----------------|--------------------------|-------------------------------|
| SEVA-A | Mater-Bi SAO31 | 138 | 19.28 |
| SEVA-B | Mater-Bi AIO5H | 141 | 2.64 |
| SEVA-C | Mater-Bi 1128RR | 146 | 0.71 |

TABLE 2. Processing Conditions for Conventional Injection Molding

| T_{inj} (°C) | T_{mould} (°C) | Flow rate (cm ³ /sec) | P_{hold} (MPa) | Cycle time (sec) |
|----------------|------------------|----------------------------------|------------------|------------------|
| 170 | 60 | 50 | 70 | 33 |

TABLE 3. Processing Conditions for Scorim

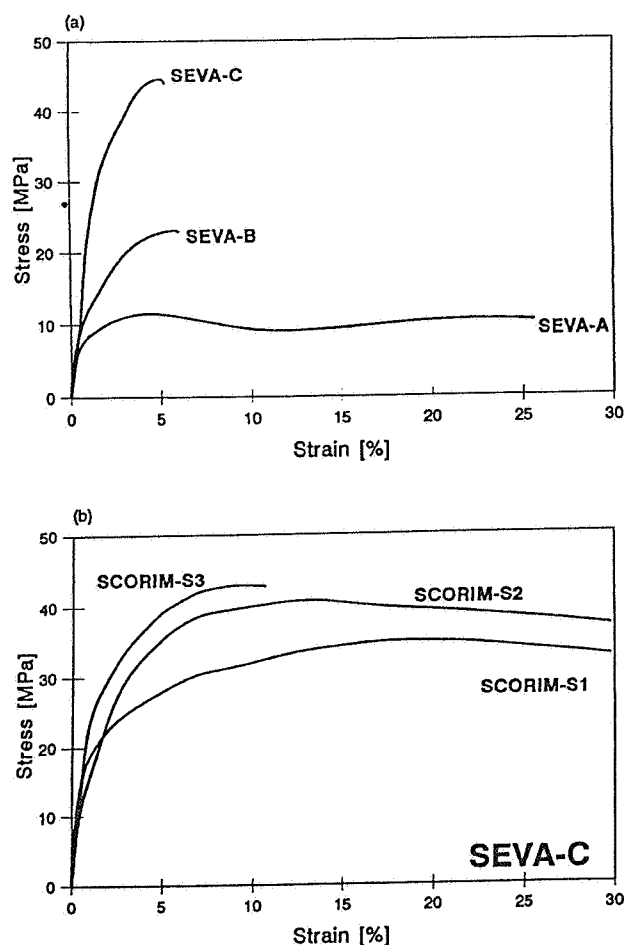
| Condition | T_{inj} (°C) | T_{mould} (°C) | P_{hold} (MPa) | t_{Scorim} (sec) | P_{max} (MPa) |
|-----------|----------------|------------------|------------------|--------------------|-----------------|
| D1 | 170 | 60 | 1.5 | 30 | 77 |
| S2 | 170 | 60 | 13 | 40 | 211 |
| S3 | 170 | 60 | 13 | 40 | 290 |

(constituted by amylose and amylopectin) with different types of monomers, including ethylene vinyl alcohol [6, 8]. They have recently become available as a mass raw material, display thermo-plastic behavior, and can be transformed by standard melt-processable techniques.

In this work, samples of starch-based polymers

TABLE 4. Results of the Tensile Tests

| Injection molding | Material | UTS (MPa) | $E_{1\%}$ (GPa) | ϵ_r (%) |
|-------------------|----------|-----------|-----------------|------------------|
| Conventional | SEVA-A | 10.5 | 0.84 | 25.6 |
| | SEVA-B | 23.1 | 1.20 | 6.0 |
| | SEVA-C | 35.6 | 1.81 | 5.3 |
| Scorim | S1 | 35.2 | 2.30 | 48.3 |
| | S2 | 38.9 | 2.02 | 35.8 |
| | S3 | 41.8 | 2.97 | 7.1 |

**FIGURE 1.** Tensile curves: (a) conventional injection molding and (b) Scorim.

were injection molded under different thermo-mechanical conditions, in order to produce moldings with a high level of anisotropy. These samples were produced by conventional injection molding and by shear controlled orientation injection molding (Scorim) [9–11]. The latter technique is based on the action of a macroscopic shear field imposed on the polymer at the melt/solid interface during solidification, providing for the control of the orientation of the macromolecules and/or filler constituents.

EXPERIMENTAL

In the present work, 60/40 (mol/mol) starch/poly(ethylene vinyl alcohol) copolymers (SEVA) were used. The starch used was obtained from native maize, with a typical composition of 70% amylopectin and 30% amylose (wt%). The three grades selected were obtained from Novamont, Italy. All the materials display a semicrystalline behavior, as has been shown previously by X-ray diffraction [12]. Their trade names, melting temperatures and melt flow indexes (MFIs) are presented in Table 1. Owing to the complex nature of these blends the characterization of their molecular weights is very difficult and rare. Useful information on the material molecular organization is mainly inferred from rheological data (e.g. [13]).

Injection-molded samples were produced on a conventional molding machine and on a machine fitted with a Scorim facility. The conventional injection-molding machine, a Krauss-Maffei KM60-120A, was used to produce ISO standard tensile bars and impact plates, in the three grades of the starch-based polymers. The 1.5 mm thick impact plates were produced in two types of geometry and gating (circular, 60 mm in diameter with a side pin gate; and square, 60 mm edge, with a film gate).

The shear-controlled injection-molding technique was used to produce tensile bars in the grade SEVA-C. These samples have a circular cross-section (5 mm in diameter) and a total length of 80 mm (with an effective testing zone of 30 mm). They were moulded on a Demag D-150 NCIII-K injection machine fitted with the Scorim equipment. The processing conditions for both techniques are presented in Tables 2 and 3.

The molding work was followed by a simulation of the injection filling stage, using the finite element package C-Flow, in order to quantify the thermo-mechanical solicitations imposed on the polymer melt for the different gating geometries used. These simulations were done for a wide range of flow rates (10–60 cm³/sec), and the values of the maximum shear stress and the maximum melt temperature were computed for a point on the vicinity of the gate. This work was based on our own thermo-rheological data, obtained by capillary rheometry and differential scanning calorimetry (DSC) analysis. An extensive material characterization may be found elsewhere [6, 7, 12].

The mechanical characterization included tensile and impact tests. Tensile experiments were performed on an Instron 4505 machine, at room

TABLE 3. Processing Conditions for Scorim

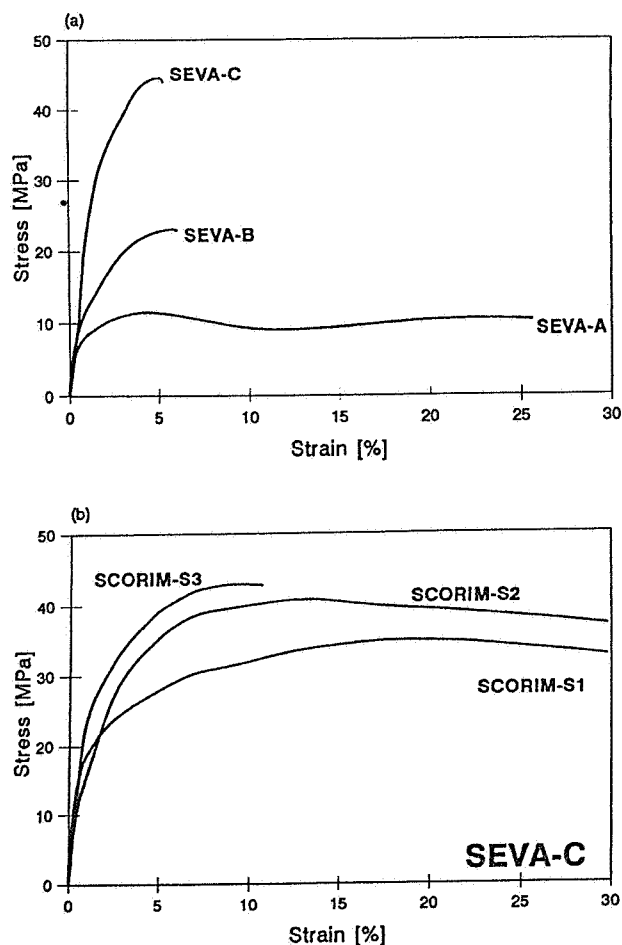
| Condition | T_{ini} (°C) | T_{mould} (°C) | P_{hold} (MPa) | t_{Scorim} (sec) | P_{max} (MPa) |
|-----------|-------------------|---------------------|---------------------|-----------------------|--------------------|
| D1 | 170 | 60 | 1.5 | 30 | 77 |
| S2 | 170 | 60 | 13 | 40 | 211 |
| S3 | 170 | 60 | 13 | 40 | 290 |

(constituted by amylose and amylopectin) with different types of monomers, including ethylene vinyl alcohol [6, 8]. They have recently become available as a mass raw material, display thermo-plastic behavior, and can be transformed by standard melt-processable techniques.

In this work, samples of starch-based polymers

TABLE 4. Results of the Tensile Tests

| Injection molding | Material | UTS (MPa) | $E_{1\%}$ (GPa) | ϵ_r (%) |
|-------------------|----------|--------------|--------------------|---------------------|
| Conventional | SEVA-A | 10.5 | 0.84 | 25.6 |
| | SEVA-B | 23.1 | 1.20 | 6.0 |
| | SEVA-C | 35.6 | 1.81 | 5.3 |
| Scorim | S1 | 35.2 | 2.30 | 48.3 |
| | S2 | 38.9 | 2.02 | 35.8 |
| | S3 | 41.8 | 2.97 | 7.1 |

**FIGURE 1.** Tensile curves: (a) conventional injection molding and (b) Scorim.

were injection molded under different thermo-mechanical conditions, in order to produce moldings with a high level of anisotropy. These samples were produced by conventional injection molding and by shear controlled orientation injection molding (Scorim) [9–11]. The latter technique is based on the action of a macroscopic shear field imposed on the polymer at the melt/solid interface during solidification, providing for the control of the orientation of the macromolecules and/or filler constituents.

EXPERIMENTAL

In the present work, 60/40 (mol/mol) starch/poly(ethylene vinyl alcohol) copolymers (SEVA) were used. The starch used was obtained from native maize, with a typical composition of 70% amylopectin and 30% amylose (wt%). The three grades selected were obtained from Novamont, Italy. All the materials display a semicrystalline behavior, as has been shown previously by X-ray diffraction [12]. Their trade names, melting temperatures and melt flow indexes (MFIs) are presented in Table 1. Owing to the complex nature of these blends the characterization of their molecular weights is very difficult and rare. Useful information on the material molecular organization is mainly inferred from rheological data (e.g. [13]).

Injection-molded samples were produced on a conventional molding machine and on a machine fitted with a Scorim facility. The conventional injection-molding machine, a Krauss-Maffei KM60-120A, was used to produce ISO standard tensile bars and impact plates, in the three grades of the starch-based polymers. The 1.5 mm thick impact plates were produced in two types of geometry and gating (circular, 60 mm in diameter with a side pin gate; and square, 60 mm edge, with a film gate).

The shear-controlled injection-molding technique was used to produce tensile bars in the grade SEVA-C. These samples have a circular cross-section (5 mm in diameter) and a total length of 80 mm (with an effective testing zone of 30 mm). They were moulded on a Demag D-150 NCIII-K injection machine fitted with the Scorim equipment. The processing conditions for both techniques are presented in Tables 2 and 3.

The molding work was followed by a simulation of the injection filling stage, using the finite element package C-Flow, in order to quantify the thermo-mechanical solicitations imposed on the polymer melt for the different gating geometries used. These simulations were done for a wide range of flow rates (10–60 cm³/sec), and the values of the maximum shear stress and the maximum melt temperature were computed for a point on the vicinity of the gate. This work was based on our own thermo-rheological data, obtained by capillary rheometry and differential scanning calorimetry (DSC) analysis. An extensive material characterization may be found elsewhere [6, 7, 12].

The mechanical characterization included tensile and impact tests. Tensile experiments were performed on an Instron 4505 machine, at room

temperature, and with a displacement rate of 8.3×10^{-4} m/sec (50 mm/min). The elongation was assessed with a resistive extensometer.

The impact analysis was based on a Rosand IFW5 instrument, with a temperature-controlled anvil. Three testing temperatures were used (-10 , 23 and 37 °C). The tests were performed with a striking velocity of 1 m/sec, using a falling dart of 25 kg with a tip radius of 20 mm. The specimens were peripherally clamped with a ring (internal diameter of 40 mm). These tests were monitored with a high-speed video system, NAC HSV-100.

The fracture surfaces were analyzed by SEM using Leica Cambridge equipment, after being coated with a very thin gold film by ion sputtering.

RESULTS

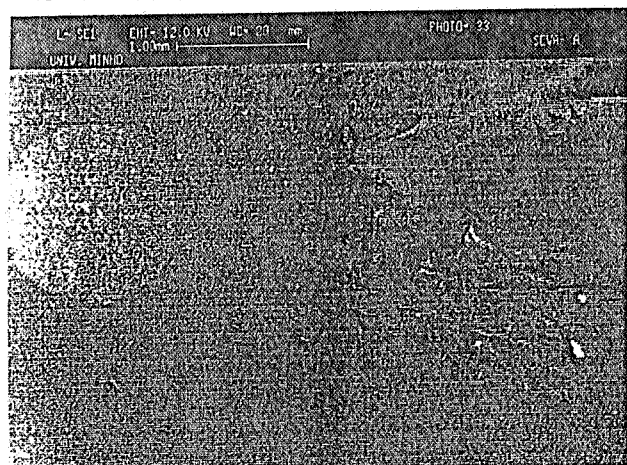
The average results of the tensile tests are presented in Table 4. Figure 1 exhibits typical stress vs strain curves for each grade (a) or Scorim condition (b). The tensile behavior was characterized by the ultimate tensile strength (UTS), the 1% secant modulus ($E_{1\%}$), the strain at break (ϵ_b) and the energy to break.

Grades SEVA-B and SEVA-C, when convention-

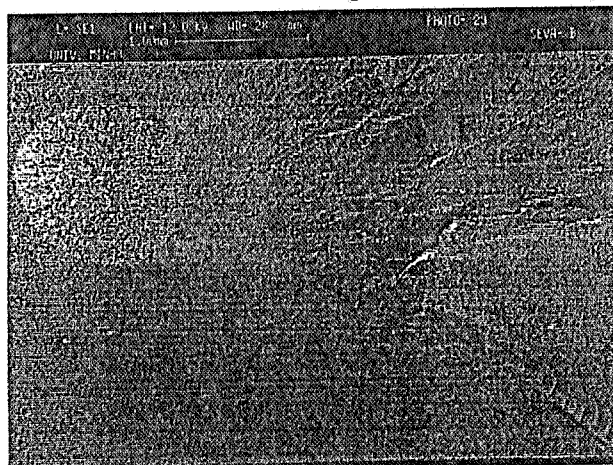
ally molded, present a brittle behavior. All the grades show a characteristic fracture morphology around a very well-defined nucleation point (Fig. 2(a)–(c)). The Scorim samples show higher ductility especially those processed with SEVA-C/S1 and S2 conditions (Fig. 1(b) and Table 4). This increment in the ductility was achieved with a simultaneous increase of stiffness, the results being deeply dependent on the pressures imposed on the melt during the Scorim cycle.

Moldings produced with SEVA-C/S3 conditions ($P_{\max}=290$ MPa) present the highest stiffness ($E_{1\%}=2.97$ GPa) but are much more brittle than other Scorim samples. However, they are slightly more ductile than conventionally molded SEVA-C. These data are confirmed by the observation of the SEM fracture surfaces. In fact, ductile fracture patterns may be observed in Fig. 3(a) and (b), contrasting with the brittle nature of Figs 2(a)–(c) and 3(c).

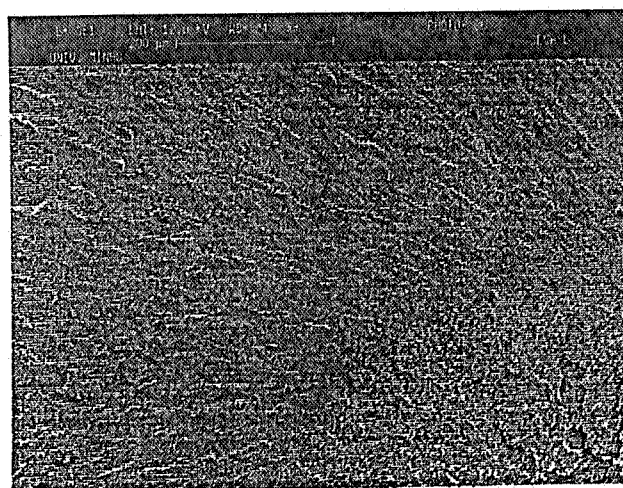
The results of the impact tests at 23 °C, summarized in Table 5, are presented in terms of the peak force (F_p), peak energy (E_p) and total failure energy (E_t). The better impact performance of the film-gated moldings is noticeable. For both gate geometries, SEVA-B discloses the higher values for F_p . Of



(a)



(b)



(c)

FIGURE 2. SEM micrographs of tensile fractures (conventional injection moulding): (a) SEVA-A; (b) SEVA-B; and (c) SEVA-C.

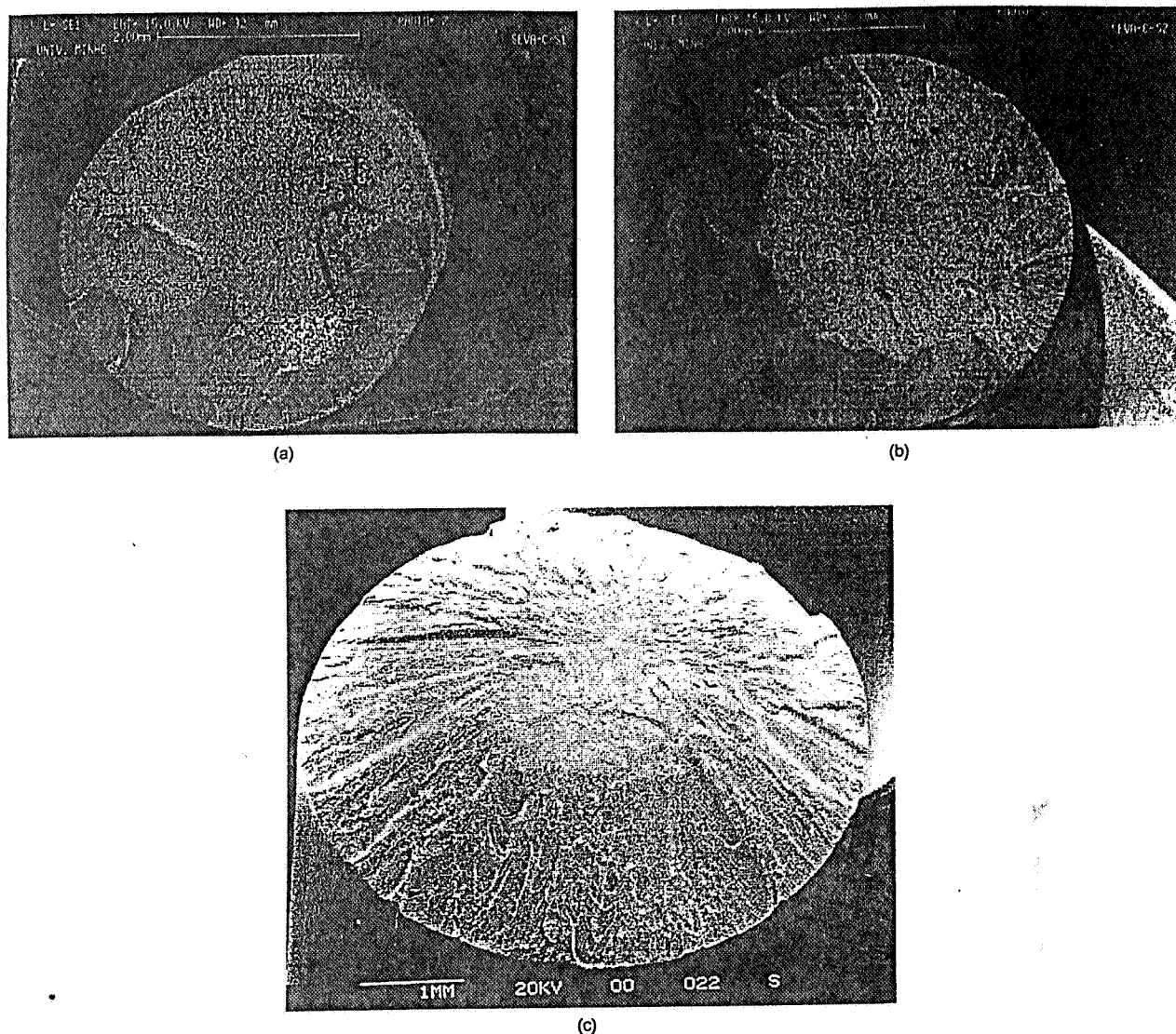


FIGURE 3. SEM micrographs of tensile fracture surfaces (Scorim): (a) SEVA-A; (b) SEVA-B; and (c) SEVA-C.

concern to the overall energy absorbed during impact (E_f) the results are, as expected, in agreement with the ductilities of the different grades. The parameter E_p presents an intermediate behavior because its values are a result of the combined effect of the impact strength (estimated by F_p) and the respective deflection of the sample.

The effect of the temperature can be observed, for SEVA-B and SEVA-C materials, in the graphs of Figs 4 and 5, respectively, for F_p and E_p . SEVA-A shows a very low strength, which does not allow for its utilization on load-bearing applications (not even on low demanding situations). As a consequence, the effect of the temperature on the impact behavior of this particular grade was not studied.

The impact data show quite a high scatter (especially for the film-gated moldings), with values of the standard error (standard deviation/average $\times 100\%$) within each batch in the range of 20%. Owing to this fact the data on Figs 4 and 5 are presented with the respective error bars. However, the fracture mode was the same for all the samples tested, featuring a characteristic star shape pattern, as can be observed in Fig. 6.

DISCUSSION

The distinct tensile behavior exhibited by the three grades tested (Fig. 1) is consistent with their different rheological behavior (flow curves and MFI) as has

TABLE 5. Impact Behavior at 23 °C

| Material | Pin-gated moldings | | | Film-gated moldings | | |
|----------|--------------------|--------------|--------------|---------------------|--------------|--------------|
| | F_p (N) | E_p (J) | E_f (J) | F_p (N) | E_p (J) | E_f (J) |
| SEVA-A | 156.0 | 0.144 | 0.780 | 203.2 | 0.178 | 0.980 |
| SEVA-B | 199.1 | 0.120 | 0.558 | 363.6 | 0.284 | 0.822 |
| SEVA-C | 195.0 | 0.083 | 0.584 | 289.2 | 0.173 | 0.731 |

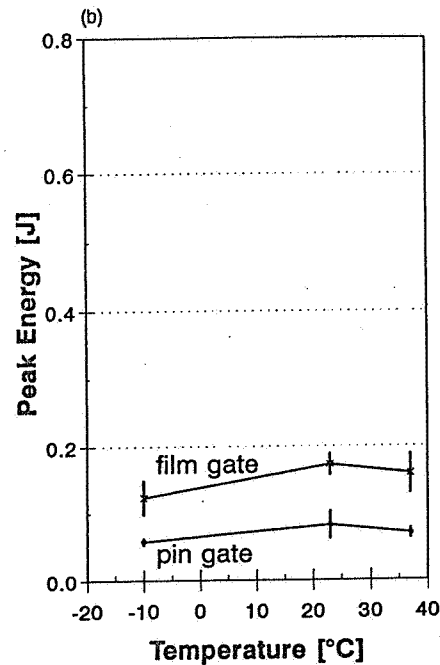
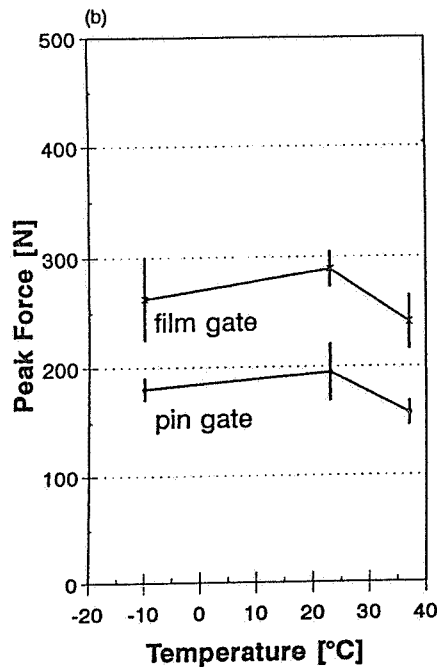
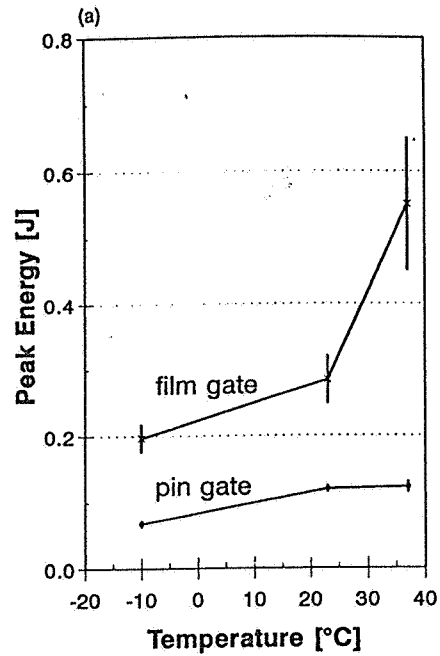
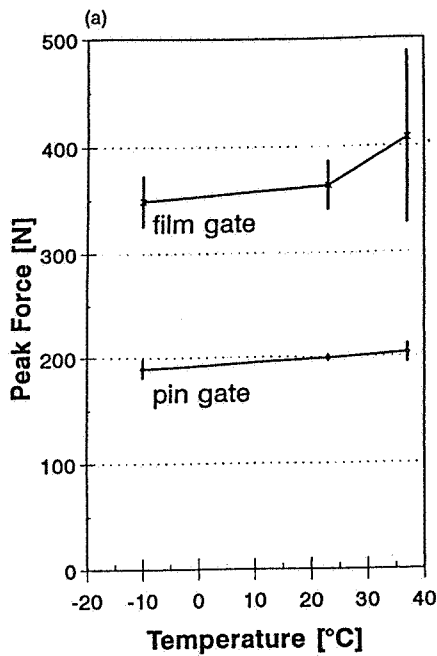


FIGURE 4. Dependence of the impact peak force on the test temperature: (a) SEVA-B and (b) SEVA-C.

been reported elsewhere [12]. As already referred to, these measurements are normally used as a qualitative assessment of the material molecular weight. For the three studied grades, MFI values are presented in Table 1 together with the determined melting temperatures.

The tensile properties of the starch-based polymers are favored by the shear field applied to the melt during the Scorim processing. The resultant higher degree of anisotropy leads to an increment in strength, stiffness and ductility. In fact, a comparison between the results obtained for Scorim and conventional moldings attests that the value of the modulus of SEVA-C could be almost double, with a slight increase of the strain at break (Scorim/S3 condition).

FIGURE 5. Dependence of the impact peak energy on the test temperature: (a) SEVA-B and (b) SEVA-C.

Alternatively, a 30% increment on the stiffness can be obtained in combination with an enhancement of the ductility by a factor of almost 10, by means of using moderate pressure during the Scorim cycle (Scorim/S1 condition).

The impact performance of these polymers (Table 5 and Figs 4 and 5) shows some unusual features. There is a reproducible influence of the gate geometry in the values of the peak force and impact energies that is more important than the effect of the testing temperature. As all the selected temperatures are below the material glass transition temperature (which is in the range of 50–55 °C), there is a negligible influence of the temperature on the obtained results (plots of Figs 4 and 5). This may

allow for the utilization of this eventually as an implant material at body temperature, and its storage in refrigerator chambers without any loss of the impact performance.

The important effect of the gate geometry should be related to the thermomechanical field imposed to the polymer in the vicinity of the gate. For the case of the pin gate, with a flow section of 0.6 mm in diameter, the polymer is submitted to a severe shear field that leads to high local heating (owing to the viscous dissipation) and mechanical damage. These assumptions were quantitatively confirmed by the results of the computational modeling of the filling of the mold cavity (Fig. 7). It is noticeable that the stress level imposed to the melt is about four times higher in the case of the pin gate. For the nominal flow rate used ($50 \text{ cm}^3/\text{sec}$) the temperature increments, owing to the flow through the runner system and the gate, are 20 and 15°C , respectively, for the pin and film gate geometries.

CONCLUSIONS

This work has shown that biodegradable starch-based copolymers have an interesting combination of mechanical properties that could meet the specifications of load-bearing biomedical applications. The results obtained allow the following main conclusions:

- (1) Shear-controlled injection molding is an effective route for gaining improvements in the mechanical properties of starch-based polymers, enabling significant increments in both stiffness and ductility.
- (2) The impact performance presents a low sensitivity to temperature (in the range from -10 to 37°C). However, the impact behavior can be adversely affected by severe local shearing imposed by the molding tool.

These promising results suggest that starch-based polymers, filled with suitable reinforcements, such as bioglass or hydroxylapatite, could be a potential alternative to biodegradable materials currently in use on biomedical applications.

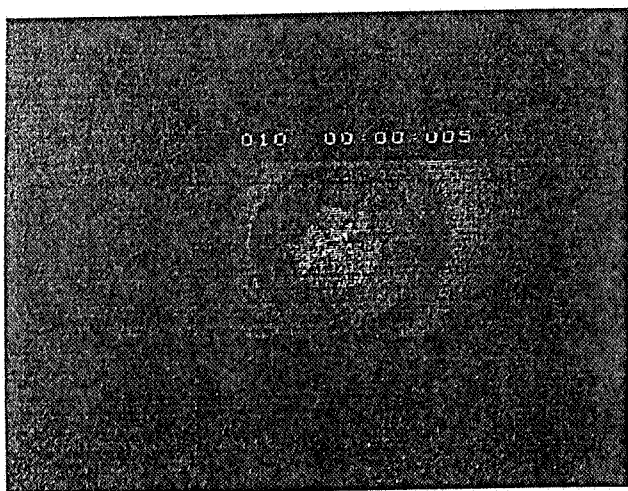


FIGURE 6. Fracture development during impact.

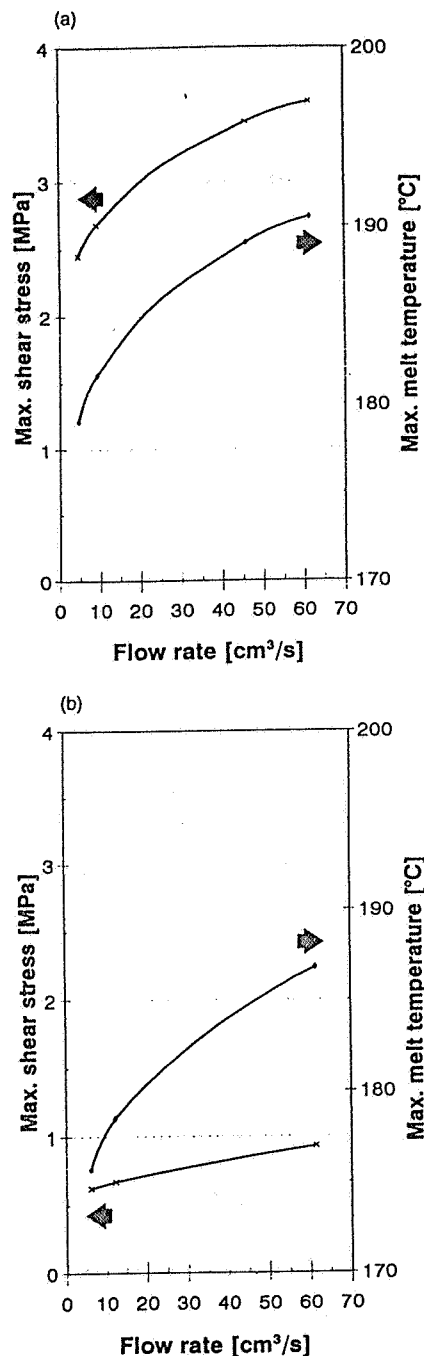


FIGURE 7. Results of computational simulations of the filling stage: (a) pin gate and (b) film gate.

REFERENCES

1. P. U. Rokkanen, *Ann. Med.*, 23, 109 (1991).
2. A. U. Danniel, K. P. Adriano, W. P. Smutz, M. K. O. Chang and J. Heller, *J. Appl. Biomater.*, 5, 51 (1994).
3. F. W. Baumgart and S. M. Perren, in *Clinical and Laboratory Performance of Bone Plates*, J. P. Harvey and R. F. Games, eds., ASTM STP1217, Philadelphia, p. 42 (1994).
4. J. C. Knowles and G. W. Hastings, *J. Mater. Sci.: Mater. Med.*, 3, 352 (1992).
5. J. C. Knowles and G. W. Hastings, *J. Mater. Sci.: Mater. Med.*, 4, 102 (1993).
6. C. Bastioli, V. Bellotti, L. Del Guidice and G. Gilli, *J. Environ. Polym. Degr.*, 1, 181 (1993).
7. Y. Yoshida and T. Uemura, *Biodegradable Plastics and*

- Polymers*, Y. Doi and K. Fukuda, eds, Elsevier Science, Tokyo, 443 (1994).
8. C. Bastioli, V. Bellotti, M. Camia, L. Del Giudice and A. Rallis, in *Biodegradable Plastics and Polymers*, Y. Doi and K. Fukuda, eds, Elsevier Science, Tokyo, p. 200 (1994).
 9. P. S. Allan and M. J. Bevis, British Patent 2170-140-B.
 10. P. S. Allan and M. J. Bevis, *Plast. Rubb. Proc. Appl.*, 7, 3 (1987).
 11. P. S. Allan and M. J. Bevis, *Comp. Manufac.*, 2, 79 (1990).
 12. R. L. Reis and A. M. Cunha, *J. Mater. Sci.: Mater. Med.*, in press: 6, 286 (1995)
 13. C. Bastioli, V. Bellotti and A. Rallis, *Rheological Acta*, 33, 307 (1994).